RSC Advances

REVIEW

View Article Online
View Journal | View Issue



Cite this: *RSC Adv.*, 2026, **16**, 21519

# Shifting paradigms: the crucial role of zeolite acid sites in dye adsorption mechanisms

Vidhya Lakshmi Gopal, [a] Monali Priyadarshini [b] and Kannan Chellapandian *[a]

Received 19th January 2026
Accepted 19th March 2026

DOI: 10.1039/d6ra00465b

rsc.li/rsc-advances

Tailoring Brønsted acid sites (BASs) and Lewis acid sites (LASs) in zeolites has become a feasible method to improve the efficiency of the adsorptive removal of dyes. Generally, in conventional approaches, textural properties, such as pore size, pore volume, and surface area, are tuned to achieve superior adsorption performances. However, these factors alone cannot guarantee robust interactions or selectivity across a broad range of dye molecules. The experimental evidences from the kinetic and isothermic data presented in this review show that adsorption is primarily influenced by the density and accessibility of acid sites. Generally, to introduce acid sites into zeolites, conventional methods, such as dealumination, acid treatment, and tuning the Si/Al ratio, are employed. However, these methods result in non-uniform distributions of acid sites, loss of crystallinity, and collapse of the framework structure under harsh treatment conditions. Modern techniques, such as atomic-layer deposition (ALD), vapor-phase metalation, and templated crystallization, can be used to overcome these limitations. This review highlights the importance of tuning acidity along with tuning textural features in zeolites for achieving effective performance in selective dye adsorption, paving the way for future developments.

## 1. Introduction

Zeolites are ordered microporous crystalline aluminosilicates that have gained significant interest in the fields of catalysis, separation process, and adsorption technologies. Due to their chemical and thermal stability, large surface area, and tunable

[a]*Department of Chemistry, Manonmaniam Sundaranar University, Abishekapatti, Tirunelveli 627 012, Tamil Nadu, India. E-mail: chellapandiankannan@gmail.com*
[b]*Center for Clean Environment, Vellore Institute of Technology, Vellore 632014, Tamil Nadu, India*

**Vidhya Lakshmi Gopal**

*Dr Vidhya Lakshmi Gopal is a doctoral researcher in the Department of Chemistry, Manonmaniam Sundaranar University, India, under the supervision of Dr C. Kannan. Her research focuses on the synthesis and acid-site engineering of zeolitic and hybrid porous materials for selective adsorption and environmental remediation. She works on tailoring Brønsted and Lewis acid sites to improve dye adsorption performance, supported by comprehensive structural and surface characterization. Her current interests include advanced zeolite modification strategies, adsorption mechanisms, and the structure–acidity–performance relationship in porous materials. She has published three papers in Q1 journals covering hybrid adsorbents, dye removal studies, and material characterization techniques.*

**Monali Priyadarshini**

*Dr Monali Priyadarshini's research focuses on developing sustainable and cost-effective wastewater treatment technologies for emerging contaminants, including dyes and pharmaceuticals. Her work integrates bio-electrochemical systems and advanced oxidation processes using waste-derived metal–organic frameworks. Emphasizing mechanistic insights, material characterization, and pollutant degradation pathways, her research aims to develop practical solutions for efficient wastewater treatment and safe effluent reuse. She has published over 30 research articles, with 1174 citations and an h-index of 16. She has received multiple best-paper presentation awards and was honored with the Inflection Award, recognizing her as a young scientist globally by Marble – Climate Tech Venture Studio, Paris.*

pore structure, these materials offer potential solutions for the sequestration of hazardous dye pollutants from industrial wastewater.[1–3] The discharge of dye waste into the environment affects aquatic systems, plants, and human health because the synthetic origin and stable aromatic structure of the dyes inhibit their biodegradation. To overcome these issues, the adsorption technique is widely used to mitigate dye effluent pollution. This approach is cost-effective compared with coagulation, precipitation, membrane filtration, and photodegradation.[4–6]

Traditionally, research on zeolite-based adsorbents has focused on textural modifications, such as increasing their pore size, pore volume, and surface area, to improve adsorption capability.[7] Although these modifications enhance accessibility and diffusion, they do not guarantee selectivity or specificity for each type of dye. Moreover, they often facilitate physisorption, which is an unstable and reversible process. For example, the larger pore and surface area of SBA-15 (Santa Barbara Amorphous-15 is a 2D material with hexagonal pore structure with a size of 2–30 nm) and MCF (Mesocellular Silica Foam is a cage-like pore structure with a size of 20–50 nm) show lower adsorption capacity compared to the smaller pore MCM-41 and MCM-48 (Mobil Composition of Matter-41 has a uniform hexagonal structure pore with a size of 2–50 nm and Mobil Composition of Matter-48 has 3D cubic structure whose diffusion strength is higher compared to MCM-41), owing to the denser acid-site of the material rather than porosity.[8] These examples suggest the disadvantages of depending only on textural optimization of zeolites rather than acid site engineering.

This has triggered a paradigm shift towards chemically driven adsorption, in which Brønsted (BAS) and Lewis acid sites (LAS) of zeolites play a crucial role in improving the selective adsorption of dye molecules. Typically, BASs are associated with bridging hydroxy groups that facilitate proton transfer, hydrogen bonding, and ion-exchange with dye molecules. On the other hand, LAS which is produced by coordinatively unsaturated metal centers and framework defects that allow strong interaction with electron-rich groups present in the dye molecules. These acid sites promote chemical interactions with dye molecules, which result in greater selectivity, a quasi-irreversible and stable process, and offers a larger adsorption capacity than physisorption.[9–11] Hence, researchers should shift their primary goal from optimizing textural properties of zeolites to acidity engineering.

Various treatments have been employed to optimize the properties of zeolites, including dealumination, acid treatment, and metal incorporation.[12–16] Nevertheless, these methods often suffer from inadequate control over the distribution of acid sites, instability in the grafted groups, and crystallinity loss after harsh treatments.[13,17] Ferrarelli *et al.*[18] reported that the non-uniform extraction of Al can often led to a heterogeneous redistribution of acid sites. Tanirbergenova *et al.*[19] observed that strong mineral acids reduced the crystallinity and collapsed the framework structure of zeolites. A study by Wang *et al.*[20] showed that metal encapsulation through grafting, impregnation, or ion exchange often lacks precise control over the placement of metals and speciation. Furthermore, Meng Liu *et al.*[21] stated that grafted non-noble-metal or extra-framework metal species may migrate, agglomerate, or leach under harsh reaction conditions, which could affect the stability of the material. These limitations have motivated the switch to modern techniques, such as atomic-layer deposition, vapor-phase metalation, templated crystallization, and confinement-controlled metal anchoring, which can be used to generate acid-site-rich zeolites without losing crystallinity or chemical structure.

Although numerous publications regarding the adsorption of dye molecules by zeolites exist, most of them predominantly concentrate on the textural modifications of zeolites for adsorption performance without acknowledging their limitations. However, to the best of our knowledge, only a few articles are available that describe how BASs and LASs in zeolites influence the adsorption process. To address this gap, this review focuses on the necessity of introducing BASs and LASs in zeolites for robust and superior adsorption performance. Based on this review, we have proposed a perspective on how acid sites bind through interaction sites of dye molecules. In addition, we have compared the kinetic and isothermic data from existing works to provide experimental support. Furthermore, this review emphasizes modern synthetic strategies for the future development of zeolites to produce stable acid-site-rich zeolites with uniform distribution of all species, without compromising their crystallinity.

**Kannan Chellapandian**

*Professor Kannan Chellapandian is an Indian chemist and academician currently serving as the Professor and Head of the Department of Chemistry at Manonmaniam Sundaranar University, Tirunelveli, Tamil Nadu. He earned his MSc in Physical Chemistry from the University of Madras and completed his PhD in Chemistry from Anna University. Prof. Kannan's research focuses on green chemistry, heterogeneous catalysis, and the synthesis and application of nanoporous solid acid catalysts for environmental and energy-related applications. He holds Indian patents in environmental and safety technologies, including a patented process for converting dye effluents into non-toxic fuel gases for effective pollution control and energy recovery, as well as a granted patent on a safety switch device to prevent LPG cylinder explosion hazards. Over his career, he has published numerous research articles in leading peer-reviewed journals, contributed to major conferences, and guided multiple PhD and MPhil scholars. His work includes developing eco-friendly catalytic materials for pollutant removal, $CO_2$ decomposition, and sustainable chemical processes, reflecting his commitment to combining fundamental chemistry with environmental solutions.*

## 2. Mechanistic insights into acid site engineering and dye–adsorbent interactions

### 2.1 BASs and LASs as key drivers for dye adsorption

The nature of the interaction between the dye molecules and the adsorbent strongly relies on the BAS/LAS of the framework rather than on the pore, and textural characteristics of zeolites.[22–24] Typically, LASs interact with the dye molecule by accepting electron pairs, while BASs do so by donating a proton to the dye molecule. This leads to the formation of a strong chemical bond between the adsorbent and adsorbate by means of complexation, coordination, deprotonation, and protonation (chemisorption), which determines selectivity (BASs/LASs select dye molecules based on the density and strength of acid sites) and specificity (BASs/LASs specifically select a functional group present in the dye molecule for stronger interaction) for the dye molecules.[25]

Generally, dye adsorption occurs at both the internal and external acid sites of the adsorbent. Initially, the dye molecules interact with the surface acid sites by means of film diffusion. Then it reaches the internal acid sites through the interconnected pore channels of the adsorbent *via* intraparticle diffusion. BASs and LASs select the dye based on the functional groups present in the molecule. The adsorption on LASs and BASs is chemisorption ($\Delta H > 40$ kJ mol$^{-1}$). Physisorption depends on surface area and is independent of BAS/LAS. In contrast, the adsorption of dye over material lacking sufficient acid sites or without acid sites are primarily governed by weaker physisorption ($\Delta H = <40$ kJ mol$^{-1}$). Stronger interactions by chemisorbed dye molecules improve the resistance to desorption in an aqueous environment. But the regeneration of a chemisorbed dye can be achieved by mild heat or chemical treatment. This is the main advantage of chemisorbed dyes on the acid sites of zeolites. In the case of physisorption, the zeolite may release the dye molecule slowly in an aqueous environment. Regeneration of the adsorbent can be done by mild heating or chemical.[23,26]

Selective functional groups on the zeolite surface enable the effective adsorption of particular dyes.[27] This selectivity allows customized adsorption of specific dyes due to the complementary chemical structure and properties of the adsorbent–absorbate interface. In contrast, the textural and pore characteristics of the zeolite may not provide the same degree of selectivity and specificity for the adsorption process. Moreover, the chemical reaction between BASs/LASs and dye molecules forms a new chemical species that binds with the zeolite surface. This may increase the overall stability of the adsorption process compared to physisorption.

### 2.2 Interaction sites in dye molecules as a key stimulant for dye adsorption

The chemical nature of the functional group in the dye molecule strongly influences its capability to adsorb onto solid-acid adsorbents. These functional groups are known as interaction sites, and they provide points of attachment to the surface of the zeolite that control the selectivity, type of interaction, and strength of adsorption. Common interaction sites in dye molecules are cationic centers, anionic centers, electron-rich donor atoms, π-conjugated atoms, and H-bonding moieties. These sites also influence the adsorption process through proton-exchange, ionic bonding, coordination bonding, electrostatic interactions, and H-bonding, as shown in Fig. 1.

Cationic centers in dye molecules can include protonated amines or quaternary ammonium groups, which primarily interact with the BASs of zeolites *via* a proton-exchange mechanism. In addition, electrostatic interactions can also occur. For example, adsorption of methylene blue,[26,28,29] and Victoria Blue[22–24] onto zeolites, and the adsorption of methylene blue and methyl violet on MXenes[29] have shown these types of interactions. Anionic centers such as sulphonate ($-SO_3^-$) or carboxylate ($-COO^-$) groups in dye molecules can be attracted to positively charged sites or metal centers of the zeolite. Studies have shown that anionic dyes like metanil yellow,[22–24] Congo red, methyl red, methyl orange, and orange G[29] interact primarily with the adsorbents through ionic interactions. Furthermore, electron-rich donors include the nitrogen of azo groups or the oxygen of carbonyl groups, coordinating with the LASs of the zeolite, which forms an inner-sphere complex. Compared to physical interactions, these interactions are more potent and selective. Some studies have suggested that adsorption through these interaction sites of the dye molecules has a stronger affinity towards the LAS, which results in a high adsorption capacity and a faster rate.[22–24,30] Some recent reviews highlighted that π–π stacking or π–cation interactions take place between the aromatic ring of the dye molecule and electron-deficient regions of the adsorbent, which promotes stronger affinity towards planar dyes.[25,31] Adsorption of dye molecules with hydroxy (–OH) and (–NH) groups is likely to form hydrogen bonds with surface hydroxy groups and adsorbed water molecules and stabilize the adsorbed dyes.[22–24,32]

Hence, the efficacy of the interaction sites present in the dye molecules relies on the number of interaction sites, the spatial arrangement, and accessibility. Furthermore, steric hindrance from a bulky substituent on the dye molecule can restrict the interaction at the adsorbent–adsorbate interface. Moreover, altering the pH and ionic strength of the dye solution leads to protonation of the functional group in the dye molecule.[33] This conversion has a substantial impact on the interactions of BASs and LASs. Therefore, the binding strength, selectivity, and stability of the adsorbent–adsorbate complex are collectively impacted by the chemical interactions rather than physical interactions. Consequently, these interaction sites are also a crucial factor for the effective removal of dyes. The various interaction types between dye functional groups and common adsorbent sites are summarized in Table 1, illustrating the complexity of dye removal mechanisms.

## 3. Experimental evidence for acid site-controlled adsorption processes

Numerous studies have demonstrated that the textural and pore characteristics of zeolites play key roles in promoting molecular

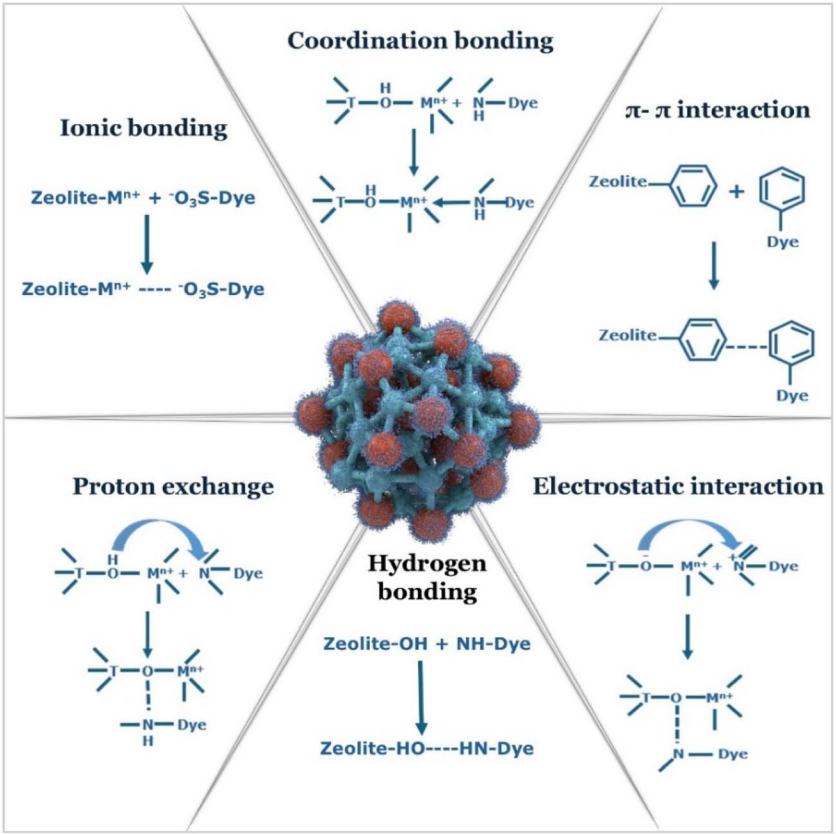


Fig. 1 Schematic representation of dye adsorption of an $M^{n+}$-modified zeolite, showing interactions of anionic dyes with LAS and metal centers, cationic dyes with BAS through hydrogen bonding and proton exchange and π–π interaction between zeolite framework and aromatic rings of the dyes.

Table 1 Representative interaction sites in dye molecules and their corresponding adsorbent sites, highlighting the interaction mechanisms involved in the adsorption processes

| Interaction site | Dye functional group | Adsorbent site | Interaction type |
|---|---|---|---|
| Cationic center | $-N^{+}R_3$, heteroaromatic cations | BASs (–OH, $H^{+}$ sites) | Proton exchange[34] and electrostatic attraction[35] |
| Azo nitrogen | –N═N– | LASs (extra-framework Al or metal centers) | Coordination and inner-sphere complexation[36] |
| Carbonyl oxygen | –C═O | LASs (extra-framework Al or metal centers) | Coordination and inner-sphere complexation[36] |
| Sulfonate | $-SO_3^{-}$ | Positively charged sites and exposed metal centers | Ionic interaction and coordination[37] |
| Carboxylate | $-COO^{-}$ | Positively charged sites or exposed metal centers | Ionic interaction and coordination[38,39] |
| Aromatic rings | $-C_6H_5$, $-C_6H_4-$ | π-deficient regions and graphitic surfaces | π–π stacking and π–cation interaction[38,40] |
| Hydroxyl | –OH | Surface hydroxyls and adsorbed water molecules | Hydrogen bonding[38] |

diffusion control while the acid sites influence the adsorption affinity and adsorption capacity.[41–45] According to hierarchical and modified zeolites, the enhanced accessibility of dye molecules to the acid sites significantly increases the adsorption capacity and selectivity.[10,46–51] Extensive studies on HY-zeolites (hydrogen form of Y-zeolite, a faujasite-type zeolite, with a 3D pore structure) with different Si/Al ratios have demonstrated robust adsorption of dyes because of their high BAS density. For example, the adsorption of methylene blue by HY (16.6) and other related HY-zeolites exhibited an adsorption capacity of ≈93 mg $g^{-1}$ at low concentration (which is close to that of commercial bentonite). This value matches the number of protonic sites, as determined by pyridine FT-IR analysis. This adsorption followed the Langmuir isotherm, which suggested that site-limited monolayer adsorption occurred rather than multilayer pore filling. In the case of kinetics, it obeyed pseudo-second-order kinetics, which indicated that the adsorption is an acid-site-controlled process[52] rather than a purely textural diffusion control.[28]

Another study proved that the controlled acid treatment of HY-zeolite (protonation/dealumination) is likely to increase the relative contribution of protonic BAS. Equilibrium was reached for the removal of mesosulfuron methyl by bare HY-zeolite at 15

 

hours, while acid-treated HY-zeolite removed it within 10 minutes. This strongly indicates that grafting BASs on the zeolite by acid treatment improves the adsorption capacity and adsorption affinity towards dye molecules. This is attributed to the creation of protonic sites in the framework, which facilitates ion exchange and electrostatic interactions. On the other hand, surface area primarily improves accessibility rather than adsorption affinity.[26] Rulan Xu *et al.* also stated that protonated zeolite shows stronger adsorption for ionic and polar molecules because of the presence of more BASs in the zeolite, which facilitates the electrostatic and acid–base interactions.[53] Since most dyes have ionic/polar functional groups, this can strengthen the interaction between the acid site and dye molecule, resulting in improved adsorption capacity.

Another study deals with the comparison of immobilization and acid treatment using clinoptilite incorporated in a polybutylene adipate (PBAT) electrospun membrane for methylene blue removal, showing that the adsorption capacity of powdered zeolite increases from ~3.3 mg $g^{-1}$ to ~4.6 mg $g^{-1}$ after 6 M HCl treatment, while that of the PBAT-zeolite membrane increases from ~8.26 mg $g^{-1}$ to 12.2 mg $g^{-1}$.[54] Conversely, a high BET surface area zeolite, such as NaX zeolite (sodium aluminosilicate with 12-membered-ring pore structure) (≈375 mg $g^{-1}$), achieved a high removal percentage for methylene blue under optimized conditions. Nevertheless, the factors such as pH, exchangeable cation/protonation site, and acid/proton availability are strong regulators for the uptake and selectivity *i.e.*, even though the textural advantages assist the adsorption, the chemical state of exchangeable cationic and protonic sites dictates whether such textural benefits are actually adsorbed under particular optimized conditions.

The adsorption capacity, as presented in Table 2, shows that higher pore size and surface area do not correlate exclusively with the adsorption capacity. Although the intraparticle diffusion and accessibility of dye molecules are regulated by the textural characteristics of the zeolite, the adsorption affinity and capacity are primarily determined by the accessibility, density, and strength of the BASs and LASs. The adsorption of methylene blue by HY-zeolite,[28] modified ZSM-5 (NZVI/SuZSM) (nanoscale zero-valent iron)[55] and NaX-zeolite[56] shows that the adsorption capacity for HY-zeolites is higher than those of ZSM-5 and NaX-zeolite. This is attributed to the typical nature of the abundant acid sites in the HY-zeolite[57] and its larger surface area. This indicated that the adsorption of methylene blue over the HY-zeolite is surface- and acid-site dependent adsorption. On the other hand, ZSM-5 also generally has stronger acid sites, but the moderate adsorption capacity is attributed to the intrinsic micropore channels, which restrict the diffusion of dye molecules into the internal acid sites, showing that the adsorption is acid-site dependent.[58] In the case of NaX-zeolite, the lower adsorption capacity is due to the presence of charge-compensating $Na^+$ ions, which reduces the BASs and weakens the interaction with the dye molecule, in addition to its lower surface area.[57] This evidence indicates that the materials with a large number of acid sites will improve adsorption efficiency even though they have lower surface areas or pore volumes.

Materials with higher numbers of BAS/LAS, such as HY-zeolite[28] and Fe-ZSM-5 (ref. 60) (Zeolite Socony Mobil-5 is a highly siliceous aluminosilicate belonging to the pentasil family with 10-membered rings), exhibited improved adsorption even with moderate or low porosity. Murat Akgül *et al.* demonstrated that desilication increased the mesoporosity of the zeolite, which promoted the adsorption performance of methylene blue. Moreover, this desilication increases BASs by decreasing the Si/Al ratio and also produces more extra-framework aluminium, which can act as LAS.[61]

In addition, steric effects around large dye molecules also influence the adsorption capacity. For example, clinoptilolite (surface area 86.85 $m^2$ $g^{-1}$ and pore volume 11.5 $cm^3$ $g^{-1}$) possesses a lower adsorption capacity (35.32 mg $g^{-1}$) for acid black 1 (anionic dye).[59] This is because clinoptilolite has limited interaction with the larger acid black 1 dye molecule.

The higher pore sizes of clinoptilite (210 nm) and NaP1 (sodium aluminosilicate with an 8-membered-ring pore structure) (70 nm) achieve adsorption capacities of 35.32 mg $g^{-1}$ and 28.44 mg $g^{-1}$, respectively.[59] Even though these materials have larger pore sizes, the adsorption capacity is relatively low since both materials have moderately low numbers of acid sites. Moreover, these larger pore structures reduce molecular sieving ability because the pore diameter becomes much larger than the molecular size of the dye molecule, leading to weaker pore-wall interaction and reduced confinement of dye molecules. This shows that the adsorption capacity is influenced by both pore/surface characteristics and the number of acid sites present in the material.

These evidences revealed that zeolites with comparable textural characteristics and increased density of acid sites demonstrated a significantly better performance for dye adsorption through stable chemical interactions. This suggested that superior adsorption performance depends on a synergistic combination of accessible pore architecture and the strength of the acid sites present in the material, rather than textural properties alone.

Although this review mainly focuses on dye pollutants, the grafting of BAS/LAS active sites can be widely used in all types of ionic and polar contaminants, including pharmaceuticals, phenolic compounds, perfluorinated sulfonates, heavy metal complexes, antibiotics, and organic acids.[62–65] For example, perfluorinated sulfonates have negatively charged sulfonate groups, which can enable them to interact with LASs in a similar way to sulfonate-containing dye molecules.[66–68] Hence, in addition to dye removal, the structure–property relationships covered in this review establish a fundamental mechanistic framework for fabricating zeolite-based adsorbents for the removal of a variety of environmental contaminants.

## 4. Synthetic routes for generating BASs and LASs in zeolites

### 4.1 Traditional methods for fabricating zeolites with BASs and LASs for selective dye adsorption

Selective dye adsorption over zeolites is strongly dependent on the distribution, strength, and accessibility of BASs and LASs. Typically, BASs are generated from bridging hydroxyl groups (Si–O–Al) through isomorphous substitution of Si with Al. LASs

Table 2 Adsorption performance (adsorption capacity, kinetic and isotherm models, and textural parameters) of zeolites and related porous adsorbents toward organic dyes. Acid site characteristics are qualitatively inferred from material type, framework chemistry (*e.g.*, Si/Al ratio, cation exchange, surface modification), or reported synthesis modifications. Direct acidity measurements were not always provided in the original studies. n.r. = not reported[a]

| Material used | Dye studied | Adsorption capacity ($q_{max}$, mg $g^{-1}$) | Kinetics followed | Isotherm followed | Pore size (nm) | Surface area ($m^2$ $g^{-1}$) | Pore volume ($cm^3$ $g^{-1}$) | Acid sites/acidity | Reference |
|---|---|---|---|---|---|---|---|---|---|
| Zeolite Y | Methyl orange | 20.62 | Pseudo-second order | Langmuir | 30.53 | 445.36 | 0.60 | Moderate Brønsted acidity | 69 |
| Zeolite Y | Eosin yellow | 52.91 | Pseudo-second order | Langmuir | 30.53 | 445.36 | 0.60 | Moderate Brønsted acidity | 69 |
| NaX zeolite | Methylene blue | 24.39 | Pseudo-second order | Langmuir | nr | 375 | 0.12 | Low Brønsted acidity | 56 |
| Clinoptilolite | Acid black 1 | 35.32 | Pseudo-second order | Freundlich | 210 | 86.85 | 11.15 | Low Brønsted acidity | 59 |
| NaP1 zeolite | Acid black 1 | 28.44 | Pseudo-second order | Langmuir | 70 | 18.33 | 80.23 | Moderate Brønsted acidity | 59 |
| HY-zeolite (2.9) | Methylene blue | 186 | Pseudo-second order | Langmuir | nr | 659 | 0.36 | High Brønsted and Lewis acidity | 28 |
| HY-zeolite (16.6) | Methylene blue | 441 | Pseudo-second order | Langmuir | nr | 631 | 0.35 | High Brønsted and Lewis acidity | 28 |
| HY-zeolite (30.0) | Methylene blue | 252 | Pseudo-second order | Langmuir | nr | 691 | 0.39 | High Brønsted and Lewis acidity | 28 |
| Fe-ZSM-5 zeolite | Basic fuchsin | 251.87 | Pseudo-second order | Langmuir | 1.93 | 399 | 0.0964 | High Brønsted acidity + Fe sites | 60 |
| Modified ZSM-5 (NZVI/SuZSM) | Methylene blue | 86.70 | Pseudo-second order | Langmuir | 2.1 | 182 | 0.48 | Brønsted + surface redox sites | 55 |
| Surfactant-modified zeolite | Crystal violet | 5.06 | Pseudo-second order | Freundlich | 21.26 | 12.67 | 0.067 | Cetylpyridinium chloride on zeolite mimics Lewis-type surface interactions | 70 |

[a] Most of the articles mainly focused on dye adsorption behaviour, isotherm, kinetics and structural/textural analysis of the zeolites rather than acidity engineering. Hence, acidity values in this table are qualitative assignments inferred from the material type, framework chemistry (*e.g.*, Si/Al ratio, cation exchange form), and reported synthesis/modification routes. In cases where the original articles did not provide direct acidity measurements (*e.g.*, pyridine-FTIR, NH-TPD, $^{31}$P NMR), acidity is interpreted based on well-established structure–acidity relationships in zeolites and mesoporous materials.

are produced by extra-framework Al species.[71,72] Hence, strategically tailoring these acid sites for improved selectivity towards the adsorption of various dye molecules is crucial, as illustrated in Fig. 2.

One of the extensively used methods to increase the concentration of acid sites is by tuning the Si/Al ratio in the framework. A low Si/Al ratio in the framework is favorable for cationic dyes, such as methylene blue, since it produces more BASs in the framework. This results in interactions between the dye molecule and BASs through a proton-exchange mechanism.[28] On the other hand, a high Si/Al ratio lowers the acidity and increases the hydrophobicity of the material.[73] Hence, this kind of material is suitable for hydrophobic dyes such as malachite green. Other than basic compositional control, dealumination is an effective approach to generate extra framework Al species, which act as LASs. Mild acid treatment can also generate additional BAS in the framework by replacing extra-framework cations such as $Na^+$, $K^+$, $Ca^{2+}$, … with $H^+$. While strong acid treatment creates defect sites that act as LAS. This type of material favors better adsorption toward azo-based dye molecules.[26,74] Post-synthetic functionalization is an alternative route for engineering acid sites by grafting sulphuric acid. This will produce a strong BAS, which is very suitable for basic dyes.[75] Conversely, grafting metal oxide[76] onto the framework and isomorphous substitution of transition-metal ions[22–24] generates LAS, which is very advantageous for anionic dyes.

Additionally, polyhedral coordination of aluminosilicate species also produces BASs and LASs in the framework.[22–24] For example, $Al_{(Td)}$ creates a negative charge in the framework, which is neutralized by the proton of (Si–O–Al) hydroxyl groups. These protons act as a BAS, while $Al_{(Ph)}$ and $Al_{(Oh)}$ create extra-framework Al species that act as a LAS. Hence, the thoughtful selection of the synthesis method, composition of the precursor, and reaction conditions is crucial to strategically increase the density of acid sites in the framework for the effective adsorption of different types of dye molecules. Table 3 summarizes the key approaches for tuning the distribution and strength of acid sites in the aluminosilicate framework.

However, these traditional methods offer a non-uniform distribution of acid sites, resulting in unstable frameworks, pore clogging, crystallinity loss, and inconsistent acid site distribution. Moreover, these classical approaches cannot independently control acid sites, hydrophobicity, and defect density. To overcome these limitations, modern strategies, such as atomic-layer deposition, vapor-phase metalation, templated crystallization, solid-state ion-exchange, and defect engineering

 

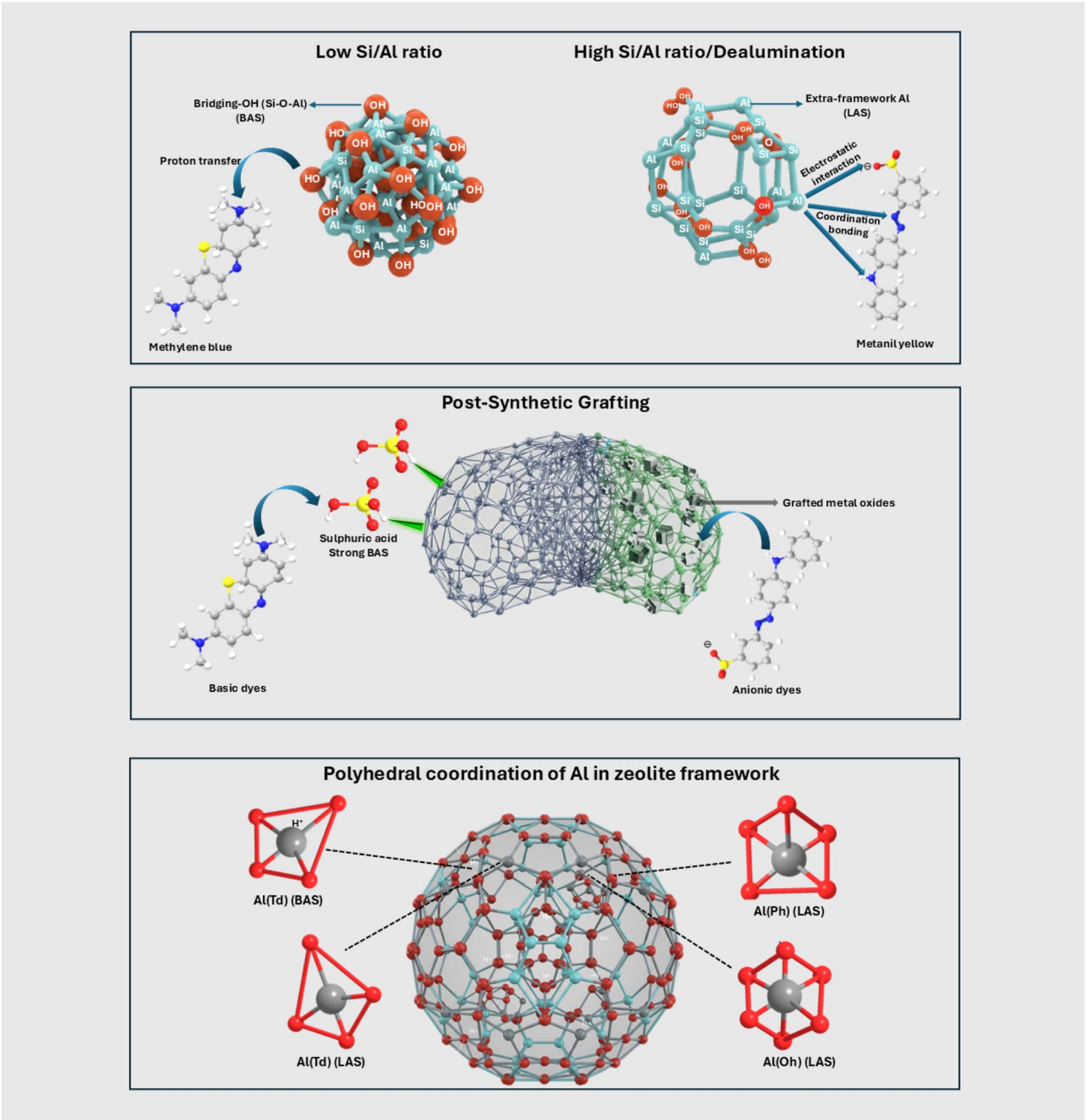


Fig. 2 Schematic of selective dye adsorption over zeolite frameworks driven by tailored acidity and composition and post-synthetic grafting. The influence of polyhedral coordination is also indicated.

techniques, are highly recommended. These sophisticated approaches improve reproducibility and homogeneity, and generate more precise BAS/LAS environments for selective dye adsorption.

### 4.2 Modern synthetic strategies to strengthen the density of BAS and LAS in zeolites without affecting framework structure or crystallinity

Increasing the density of BAS and LAS in zeolites without losing their crystallinity and structural integrity is the major challenge in the development of an effective adsorbent. Hence, modern strategies are used to improve acid-site density and accessibility with atomic-scale precision while avoiding harsh treatment.

Atomic-layer deposition (ALD) is one of the most controlled methods for integrating LASs into zeolites while maintaining crystallinity. This technique proceeds through self-limiting surface reactions to deposit metal or metal oxide species on the internal or external surface of the zeolite with angstrom-level precision. When ALD is optimized, it introduces highly dispersed species based on Zr, Ti, Sn, or Fe that act as LAS,

Table 3 Strategies for tailoring BASs and LASs in aluminosilicates to improve selective dye adsorption[a]

| Strategy | Effect on acid sites | Interaction with dye molecules | References |
|---|---|---|---|
| Si/Al ratio tuning | Low Si/Al ratio produces higher BAS density; whereas high Si/Al ratio generates lower acidity and higher hydrophobicity | BASs protonate cationic dyes *via* proton-exchange, whereas hydrophobic zeolites favour the adsorption of dyes with bulky aromatic rings | 28 and 77 |
| Dealumination (acid treatment) | Mild acid treatment generates BASs by $H^+$ exchange; severe acid treatment removes Al from the framework and forms extra-framework Al, which forms LAS | BASs favour the adsorption of cationic/azo dyes *via* protonation; LASs improve interaction with electron-donating groups in azo dyes | 12, 14–16 and 78 |
| Post-synthetic functionalization | Sulfonic acid grafting produces strong BAS, while metal oxide grafting ($TiO_2$, $Fe_2O_3$, and $CeO_2$) produces strong LAS | BASs promote the adsorption of basic dyes *via* protonation, and LASs enable π–π/electron donor–acceptor interactions with azo dyes | 31 and 75 |
| Isomorphous substitution (transition metals) | Introduces LASs *via* framework/extra-framework transition metals (Fe, Co, Ni, La) | LASs coordinate with anionic dyes *via* electron pair donation and ion–dipole interactions | 22–24 and 79 |
| Polyhedral coordination of Al species | Al in tetrahedral ($Al^4$) sites creates BASs *via* bridging OH groups; octahedral/pentahedral Al generates extra-framework species and forms LAS | BASs protonate the cationic dyes; LASs bind anionic/azo dyes through coordination with sulfonate or azo groups | 22–24 |

[a] Most of the articles focused on dye adsorption behaviour, isotherm, kinetics and structural/textural analysis of the zeolites, rather than acidity engineering. Based on the literature, these strategies are anticipated to impact dye adsorption through the acid sites present on the zeolite framework, although direct dye adsorption experiments were not reported in some cases.

without aggregating into particles that block the pores or collapse the porous structure. For instance, Yang *et al.* demonstrated that this technique can be used to deposit oxide species onto the porous support to create well-dispersed LASs without collapsing the structure.[80]

Vapor-phase metalation broadens this idea by employing metal halides or volatile organometallic precursors, which diffuse into the pores of the zeolite without being exposed to liquid-phase hydrolysis, since it causes dealumination. This technique allows the metal to penetrate deeper into pores to form a hierarchical framework or mesoporous structure. This results in uniform, spatially distributed LASs with higher crystallinity. Valeryia Kasneryk *et al.* demonstrated a zeolite formed by using this approach with stable crystalline layers and crystal structure.[81]

Templated crystallization offers a bottom-up approach to customize both acidity and accessibility, specifically by surfactant-templated and organometallic-mediated synthesis.[82–85] Surfactant-templated synthesis creates a lamellar structure with mesopores that offers a higher percentage of crystallinity of acid sites on the external surface of the zeolite.[86] On the other hand, the organosilane-mediated method allows the transport of heteroatoms into the developing framework, which leads to the formation of BASs and LASs during crystallization. These approaches are extremely useful for dye adsorption, since the molecular size of the adsorbate frequently limits access to traditional micropores.[87] Recent studies have shown that these approaches maintain the structural order even after extended catalytic cycling. This indicates that these methods can develop hierarchical zeolites with accessibility, diffusion routes, increased acid sites, and crystallinity.[88]

Isomorphous or controlled heteroatom substitution is one of the most efficient methods for producing LASs in internal layers of the zeolite. Incorporating $Sn^{4+}$, $Zr^{4+}$, $Ti^{4+}$, or $Ga^{3+}$ into the tetrahedral framework yields clearly distinct LASs with a homogeneous electronic environment and high resistance to leaching.[89] Sn-beta and Ti-beta zeolites synthesized by this method have significant LASs without losing their crystallinity due to framework substitution.[89] Modern synthesis approaches prioritize precursor hydrolysis and condensation kinetics over phase segregation. For example, Hongwei Zhang stated that paired Sn sites in the framework create stronger LAS in Sn-beta. Because the acidity of such zeolites is intrinsic and stable under aqueous condition during dye adsorption.[90]

In parallel, solid-state ion exchange (SSIE) is one of the most useful techniques to generate BASs in zeolites without damaging the framework. To produce bridging Si–O–Al, this technique substitutes $Na^+$ or $K^+$ with $NH_4^+$, followed by calcination under controlled conditions.[91] Unlike liquid-phase strong-acid treatments, SSIE suppresses framework hydrolysis to avoid loss of crystallinity and preserves the Al coordination environment. According to recent studies, the SSIE technique provides H-form of zeolites, which have superior BAS density, minimal pore collapse, and outstanding structural retention.[92]

On the other hand, defect engineering is an advanced method for maximizing acidity and maintaining the framework structure. Framework defects, such as silanol nest and vacancy sites, can act as anchoring sites for controlled metal introduction. Effective methods to control these defects are fluoride-

 

mediated crystallization, controlled hydrolysis recondensation, and targeted silylation; each method provides a unique way for structural retention.

Fluoride-mediated synthesis is one of the best bottom-up approaches to minimize framework defects from the beginning. Fluoride anions act as a mineralizer that temporarily coordinates to the silicate oligomer, reducing the condensation barriers that favor the formation of a fully condensed Si–O–Si network with minimal defects.[93] For instance, Muhammad Ali Shah showed that the crystallization time of a zeolite is reduced significantly upon increasing fluoride incorporation, and decreased defects in the ($Si–O^-$) group.[94]

Controlled hydrolysis-recondensation is an effective top-down approach for modifying the pristine framework after synthesis, such as relocating aluminium, creating silanol nests, and removing extra-framework species. Si–O–Si or Si–O–Al can undergo hydrolysis under steaming or mild acid or base treatment, yielding silanol groups and vacancies, followed by recondensation, which might repair defects (restoring Si–O–Si) or reorganize the local framework (relocate Al).[95] The balance between repairing and defect generation is influenced by pH, temperature, time, and water activity. Systematic post-synthetic treatments, such as mild acid treatment or steaming followed by controlled drying or resiliconization, have been employed to repair defects in the framework. This also preserves crystallinity, porosity, and thermal stability and prevents structural collapse.

Targeted silylation is another route to maintain the crystallinity and crystal structure using organosilicon reagents such as chlorosilane. This reagent selectively caps silanol (Si–OH) sites to produce (Si–O–$SiR_3$) links, which will effectively passivate the defects.[96–98] Silanol nest engineering is also the best technique for controlled acid-site creation and metal anchoring. This method is based on combining all the above strategies, specifically controlled hydrolysis-recondensation (for controlled density of silanol nests), followed by silylation (to passivate defects) and subsequent metal deposition to produce well-separated LAS while also retaining the BAS framework and structural reliability. In a recent study, a self-pillared Zr-zeolite with strong LAS, which was synthesized by combining controlled Zr-grafting followed by $HNO_3$ treatment, was subjected to selective deboration to obtain silanol nests, directing the migration of surface Zr species into framework-confined sites.[99]

## 5. Conclusions and suggestions

This review highlighted the paradigm shifts in the adsorption process by addressing the key role of BAS and LAS in the zeolite over traditional textural properties. The adsorption of dye molecules is governed by multiple factors, including density, strength and accessibility of acid sites, as well as by the steric hindrance of the dye molecules and the experimental adsorption conditions. Materials lacking acid sites undergo weaker physisorption, where the adsorption is largely dependent on surface area/pore features. In the case of materials having sufficient acid sites, the adsorption is controlled by the strength and density of the acid sites. But the adsorption of dye molecules follows the same transport and diffusion mechanism in both cases. Hence, the existence and accessibility of BASs/LASs are crucial for determining adsorption affinity, selectivity and equilibrium capacity, even though the textural properties facilitate molecular transport. Additionally, this review critically analyzed both traditional and modern methods for tuning acid sites in the zeolites. Traditional zeolites often affect the crystallinity, framework structure, and homogeneous distribution of acid sites. However, advanced modern methods provide atomic-scale precision to promote the acid-site density and accessibility while preserving structural integrity and crystallinity.

Hence, this review concludes that the most promising approach for creating high-performance adsorbents is the strategic tailoring of the framework by introducing acid sites and optimizing the pore structure to achieve superior adsorption performance. Based on these observations, this review suggests that the fabrication of integrated zeolite-based composites with customized acid/active sites and comparable pore architecture can enhance the interactions with functional groups present on dye molecules. Moreover, these types of adsorbents can be applicable for the removal of all kinds of environmental contaminants.

## Author contributions

Vidhya Lakshmi Gopal contributed to the writing of the original draft, participated in discussions, and made corrections. Monali Priyadarshini and Kannan Chellapandian were involved in manuscript corrections and discussions.

## Conflicts of interest

The authors declare that there is no conflict of interest.

## Data availability

No primary research results, software or code have been included and no new data were generated or analysed as part of this review.

## Acknowledgements

This research work was supported by the Anusandhan National Research Foundation (ANRF) under the Partnerships for Accelerated Innovation and Research (PAIR) project, Government of India, sanction order ANRF/PAIR/2025/000011/PAIR-B.

## References

1 Y. S. Ho, J. C. Y. Ng and G. McKay, *Sep. Purif. Methods*, 2000, **29**, 189–232.
2 Z. Wang, T. Li, Y. Jiang, O. Lafon, Z. Liu, J. Trébosc, A. Baiker, J. P. Amoureux and J. Huang, *Nat. Commun.*, 2020, **11**, 9–17.
3 Z. Wang, Y. Jiang, A. Baiker and J. Huang, *Acc. Chem. Res.*, 2020, **53**(11), 2648–2658.

4 G. Crini, *Bioresour. Technol.*, 2006, **97**, 1061–1085.
5 A. Demirbas, *J. Hazard. Mater.*, 2009, **167**, 1–9.
6 P. N. T. Robinson, G. McMullan and R. Marchant, *Bioresour. Technol.*, 2001, **77**, 247–255.
7 F. Bahmanzadegan and A. Ghaemi, *J. Hazard. Mater. Adv.*, 2025, **17**, 100617.
8 H. I. Meléndez-Ortiz, B. Puente-Urbina, J. A. Mercado-Silva and L. García-Uriostegui, *Int. J. Appl. Ceram. Technol.*, 2019, **16**, 1533–1543.
9 Y. Chu, X. Yi, C. Li, X. Sun and A. Zheng, *Chem. Sci.*, 2018, **9**, 6470–6479.
10 S. T. Pham, M. B. Nguyen, G. H. Le, T. D. Nguyen, C. D. Pham, T. S. Le and T. A. Vu, *Chemosphere*, 2021, **265**, 129062.
11 Q. Zhao, W.-H. Chen, S.-J. Huang, Y.-C. Wu, H.-K. Lee and S.-B. Liu, *J. Phys. Chem. B*, 2002, **106**, 4462–4469.
12 M. Ibáñez, E. Epelde, A. T. Aguayo, A. G. Gayubo, J. Bilbao and P. Castaño, *Appl. Catal., A*, 2017, **543**, 1–9.
13 A. Palčić and V. Valtchev, *Appl. Catal., A*, 2020, **606**, 117795.
14 L. K. Anh, T. T. Q. Nhu, L. T. T. Hien, N. T. Thong, N. T. T. Phuong, N. Van Dung, N. T. H. Duong and N. Q. Long, *Int. J. Environ. Sci. Technol.*, 2025, **22**, 12763–12780.
15 L. Zhang, J. Chen, X. Guo, S. Yin, M. Zhang and Z. Rui, *Catal. Today*, 2021, **376**, 119–125.
16 W. Wang, W. Zhang, Y. Chen, X. Wen, H. Li, D. Yuan, Q. Guo, S. Ren, X. Pang and B. Shen, *J. Catal.*, 2018, **362**, 94–105.
17 L. C. Juang, C. C. Wang and C. K. Lee, *Chemosphere*, 2006, **64**, 1920–1928.
18 G. Ferrarelli, M. Migliori and E. Catizzone, *ACS Omega*, 2024, **9**, 29072–29087.
19 S. Tanirbergenova, D. Tugelbayeva, N. Zhylybayeva, A. Aitugan, K. Tazhu, G. Moldazhanova and Z. Mansurov, *Processes*, 2025, **13**(9), 2896–2915.
20 H. Wang, L. Wang and F.-S. Xiao, *ACS Cent. Sci.*, 2020, **6**, 1685–1697.
21 M. Liu, C. Miao and Z. Wu, *Ind. Chem. Mater.*, 2024, **2**, 57–84.
22 V. L. Gopal and K. Chellapandian, *Environ. Res.*, 2023, **220**, 115111.
23 V. L. Gopal and C. Kannan, *Environ. Sci. Pollut. Res.*, 2023, **30**, 67788–67803.
24 V. L. Gopal and K. Chellapandian, *Surf. Interfaces*, 2023, **40**, 103113.
25 F. Bahmanzadegan and A. Ghaemi, *J. Hazard. Mater. Adv.*, 2025, **17**, 100617.
26 T. Kasmi-Belouzir, A. Soualah, K. Kouachi, S. Mignard and I. Batonneau-Gener, *J. Environ. Health Sci. Eng.*, 2021, **19**, 1435–1445.
27 T. Bień, D. Kołodyńska and W. Franus, *Materials*, 2021, **14**(24), 7817.
28 T. Kasmi, A. Soualah, S. Mignard and I. Batonneau-Gener, *J. Environ. Health Sci. Eng.*, 2018, **16**, 239–247.
29 S. Lim, J. H. Kim, H. Park, C. Kwak, J. Yang, J. Kim, S. Y. Ryu and J. Lee, *RSC Adv.*, 2021, **11**, 6201–6211.
30 M. Zeeshan, T. Javed, C. Kumari, A. Thumma, M. Wasim, M. B. Taj, I. Sharma, M. N. Haider and M. Batool, *Sustainable Chem. Environ.*, 2025, **9**, 100217.
31 A. Hamd, M. Shaban, G. M. Al-Senani, M. N. Alshabanat, A. Al-Ghamdi, A. R. Dryaz, S. A. Ahmed, R. El-Sayed and N. K. Soliman, *Sci. Rep.*, 2023, **13**, 1–17.
32 A. A. Kouzoutzoglou-Efremidou, A. K. Tolkou, K. N. Maroulas, R. I. Kosheleva, I. A. Katsoyiannis and G. Z. Kyzas, *Langmuir*, 2025, **41**, 3603–3622.
33 S. Karmaker, M. N. Uddin, H. Ichikawa, Y. Fukumori and T. K. Saha, *J. Environ. Chem. Eng.*, 2015, **3**, 583–592.
34 Z. Xu, T. Fu, Y. Han, Z. Li and G. Zhan, *Fuel*, 2023, **349**, 128671.
35 M. Trachta, O. Bludský, J. Vaculík, R. Bulánek and M. Rubeš, *Sci. Rep.*, 2023, **13**, 12380.
36 P. Gu, K. Li and H. Su, *Sep. Purif. Technol.*, 2025, **364**, 132448.
37 M. Heravi, V. Srivastava, V. Zeynali and M. Sillanpää, *Environ. Sci. Pollut. Res.*, 2024, **31**, 1–22.
38 S. Guo, Z. Zou, Y. Chen, X. Long, M. Liu, X. Li, J. Tan and R. Chen, *Environ. Pollut.*, 2023, **320**, 121060.
39 Y. Fang, A. Zhou, W. Yang, T. Araya, Y. Huang, P. Zhao, D. Johnson, J. Wang and Z. J. Ren, *Sci. Rep.*, 2018, **8**, 229.
40 V. A. Tran, K. B. Vu, T. T. T. Vo, V. T. Le, H. H. Do, L. G. Bach and S. W. Lee, *Appl. Surf. Sci.*, 2021, **538**, 148065.
41 K. G. Strohmaier, in *Zeolites and Catalysis*, 2010, pp. 57–86.
42 P. A. Wright and G. M. Pearce, in *Zeolites and Catalysis*, 2010, pp. 171–207.
43 J. Pérez-Pariente, R. García, L. Gómez-Hortigüela and A. B. Pinar, in *Zeolites and Catalysis*, 2010, pp. 107–129.
44 C.-Y. Chen and S. I. Zones, in *Zeolites and Catalysis*, 2010, pp. 155–170.
45 S.-E. Park and N. Jiang, in *Zeolites and Catalysis*, 2010, pp. 131–153.
46 C. H. Christensen, K. Egeblad, C. H. Christensen and J. C. Groen, *Chem. Soc. Rev.*, 2008, 2530–2542.
47 Y. Feng, H. Zhou, G. Liu, J. Qiao, J. Wang, H. Lu, L. Yang and Y. Wu, *Bioresour. Technol.*, 2012, **125**, 138–144.
48 M. Goswami and P. Phukan, *J. Environ. Chem. Eng.*, 2017, **5**, 3508–3517.
49 M. Naushad, A. A. Alqadami, A. A. Al-Kahtani, T. Ahamad, M. R. Awual and T. Tatarchuk, *J. Mol. Liq.*, 2019, **296**, 112075.
50 A. M. Aldawsari, I. H. Alsohaimi, A. A. Al-Kahtani, A. A. Alqadami, Z. E. A. Abdalla and E. A. M. Saleh, *Sep. Sci. Technol.*, 2021, **56**, 835–846.
51 A. G. Tafti, A. Rashidi, H.-A. Tayebi and M. E. Yazdanshenas, *Int. J. Nano Dimens.*, 2018, **9**, 79–88.
52 Y. S. Ho and G. McKay, *Process Biochem.*, 1999, **34**, 451–465.
53 R. R. Xu, W. Pang, J. Yu, Q. Huo and J. Chen, *Chemistry of Zeolites and Related Porous Materials: Synthesis and Structure*, 2010, DOI: 10.1002/9780470822371.
54 D. Picón, A. Vergara-Rubio, S. Estevez-Areco, S. Cerveny and S. Goyanes, *Molecules*, 2023, **28**(1), 81, DOI: 10.3390/molecules28010081.
55 A. K. Hammed, N. Dewayanto, D. Du, M. H. Ab Rahim and M. R. Nordin, *J. Environ. Chem. Eng.*, 2016, **4**, 2607–2616.
56 H. H. Aya, N. Djamel, A. Samira, M. Otero and M. A. Khan, *RSC Adv.*, 2024, **14**, 23816–23827.
57 D. W. Breck, *Anal. Chim. Acta*, 1975, **75**, 493.

58 J. A. Martens, *Synthesis of High-Silica Aluminosilicate Zeolites*, Elsevier: Distributors for the U.S. and Canada, Elsevier Science Pub. Co., 1987, vol. 33.
59 A. Dzieniszewska, M. Pajak and J. K. Komosińska, *Molecules*, 2025, **30**, 1677.
60 B. Ba Mohammed, A. Hsini, Y. Abdellaoui, H. A. Oualid, M. Laabd, M. El Ouardi, A. A. Addi, K. Yamni and N. Tijani, *J. Environ. Chem. Eng.*, 2020, **8**, 104419.
61 M. Akgül and A. Karabakan, *Microporous Mesoporous Mater.*, 2011, **145**, 157–164.
62 R. E. Kukwa and S. E. Dann, *Desalin. Water Treat.*, 2019, **153**, 136–144.
63 Y. Huang, H. Zhang, L. Gao, T. Yan, Y. Yan, Y. Zhang and Y. Tang, *Microporous Mesoporous Mater.*, 2022, **341**, 112110.
64 I. Braschi, S. Blasioli, L. Gigli, C. Gessa, A. Alberto and A. Martucci, *J. Hazard. Mater.*, 2010, **178**, 218–225.
65 C. A. Ponge, D. R. Corbin, C. M. Sabolay and M. B. Shiflett, *Ind. Chem. Mater.*, 2024, **2**, 270–275.
66 V. Ochoa-Herrera and R. Sierra-Alvarez, *Chemosphere*, 2008, **72**, 1588–1593.
67 A. V. Alves, M. Tsianou and P. Alexandridis, *Chemosphere*, 2025, **378**, 144414.
68 N. Khodabakhshloo and B. Biswas, *Appl. Clay Sci.*, 2023, **244**, 107101.
69 A. A. Adeyemo, I. O. Adeoye and O. S. Bello, *Appl. Water Sci.*, 2017, **7**, 543–568.
70 A. Bagheri, S. H. Khabbaz and A. A. Rafati, *Sci. Rep.*, 2024, **14**, 1–18.
71 M. Nielsen, R. Y. Brogaard, H. Falsig, P. Beato, O. Swang and S. Svelle, *ACS Catal.*, 2015, **5**, 7131–7139.
72 J. Dedecek, Z. Sobalik and B. Wichterlova, *ChemInform*, 1996, **27**(7), DOI: 10.1002/chin.201239221.
73 L. Boudjema, M. Assaf, F. Salles, P.-M. Gassin, G. Martin-Gassin and J. Zajac, *Molecules*, 2024, **29**, 2952.
74 D. S. P. Handoko, *Formosa J. Sci. Technol.*, 2023, **2**, 363–378.
75 C.-Y. Chen and S. I. Zones, in *Zeolites and Catalysis*, 2010, pp. 155–170.
76 V. A. R. Villegas, J. I. De León Ramirez, L. Pérez-Cabrera, S. Pérez-Sicairos, R. I. Yocupicio-Gaxiola, J. R. Chávez-Méndez, L. Huerta-Arcos and V. Petranovskii, *Mater. Chem. Phys.*, 2025, **331**, 130199.
77 E. Von-Kiti, W. O. Oduro, M. A. Animpong, K. Ampomah-Benefo, G. Boafo-Mensah, B. Kwakye-Awuah and C. D. Williams, *Heliyon*, 2023, **9**, e20049.
78 M. Nielsen, R. Y. Brogaard, H. Falsig, P. Beato, O. Swang and S. Svelle, *ACS Catal.*, 2015, **5**, 7131–7139.
79 P. Wu, T. Komatsu and T. Yashima, *Microporous Mesoporous Mater.*, 1998, **20**, 139–147.
80 W. Yang, X. Liu, L. A. O'Dell, X. Liu, L. Wang, W. Zhang, B. Shan, Y. Jiang, R. Chen and J. Huang, *JACS Au*, 2023, **3**, 2586–2596.
81 V. Kasneryk, M. Shamzhy, J. Zhou, Q. Yue, M. Mazur, A. Mayoral, Z. Luo, R. E. Morris, J. Čejka and M. Opanasenko, *Nat. Commun.*, 2019, **10**, 5129.
82 D. Kerstens, B. Smeyers, J. Van Waeyenberg, Q. Zhang, J. Yu and B. F. Sels, *Adv. Mater.*, 2020, **32**, 2004690.
83 R. Bai, Y. Song, Y. Li and J. Yu, *Trends Chem.*, 2019, **1**, 601–611.
84 X. Jia, W. Khan, Z. Wu, J. Choi and A. C. K. Yip, *Adv. Powder Technol.*, 2019, **30**, 467–484.
85 K. Möller and T. Bein, *Chem. Soc. Rev.*, 2013, **42**, 3689–3707.
86 M. Hartmann, M. Thommes and W. Schwieger, *Adv. Mater. Interfaces*, 2021, **8**, 2001841.
87 H. Xin, X. Li, L. Chen, Y. Huang, G. Zhu and X. Li, *Energy Environ. Focus*, 2013, **2**, 18–40.
88 O. V. Shvets, M. M. Kurmach, K. M. Konysheva, O. I. Lozovytska and N. D. Shcherban, *Mater. Today Chem.*, 2024, **36**, 101921.
89 A. Corma, L. T. Nemeth, M. Renz and S. Valencia, *Nature*, 2001, **412**, 423–425.
90 H. Zhang, I. b. Samsudin, S. Jaenicke and G. K. Chuah, *Catal. Sci. Technol.*, 2022, **12**, 6024–6039.
91 S. Zhang, J. Chen, Y. Meng, L. Pang, Y. Guo, Z. Luo, Y. Fang, Y. Dong, W. Cai and T. Li, *Appl. Surf. Sci.*, 2022, **571**, 151328.
92 C. Li, T. Li, Q. Cui, T. Wang, C. Wang, J. Yang, J. Shi, X. Bao and Y. Yue, *Phys. Chem. Chem. Phys.*, 2025, **27**, 15819–15834.
93 K. C. Kemp, Ö. F. Altundal, D. Jo, W. Huang, Q. Wang, F. Deng, G. Sastre and S. B. Hong, *Chem. Sci.*, 2025, **16**, 7579–7589.
94 M. A. Shah, T. Nagornyy, S. E. Aiwekhoe, S. Hong, N. H. H. Tran, S. Luo, Z. Chen, S. M. Auerbach and W. Fan, *Cryst. Growth Des.*, 2025, **25**, 1821–1832.
95 J. Yang and E. G. Wang, *Curr. Opin. Solid State Mater. Sci.*, 2006, **10**, 33–39.
96 R. Singh and P. K. Dutta, *Microporous Mesoporous Mater.*, 1999, **32**, 29–35.
97 R. Liu, S. Zeng, T. Sun, S. Xu, Z. Yu, Y. Wei and Z. Liu, *ACS Catal.*, 2022, **12**, 4491–4500.
98 H.-T. Vu, F. M. Harth and N. Wilde, *Front. Chem.*, 2018, **6**, 143.
99 M. Zhang, C. Zhong, H. Wu, X. Yan, S. Yan, J. Han, X. Wang, J. Liu and L. Ren, *Inorg. Chem.*, 2025, **64**, 17045–17057.